

b and $\chi(\gamma_1) = 2\binom{k}{a}\binom{k}{b}$ if $a \neq b$. The numbers $\chi(\gamma_2)$, $\chi(\gamma_3)$, and $\chi(\gamma_4)$ differ for each reaction kind and may be counted by simple combinatorial considerations.

For the reaction kind $A \rightleftharpoons B$ ($a = 1, b = 1$):

$$\binom{k}{1} = k \quad \chi(\gamma_2) = 0 \quad \chi(\gamma_3) = \chi(\gamma_4) = k$$

$$t = (k^2 + k + k)/4 = k(k+2)/4$$

For the reaction kind $A + X \rightleftharpoons B$ ($a = 1, b = 2$):

$$\binom{k}{1} = k \quad \binom{k}{2} = k(k-1)/2 \quad \chi(\gamma_2) = \chi(\gamma_3) = \chi(\gamma_4) = 0$$

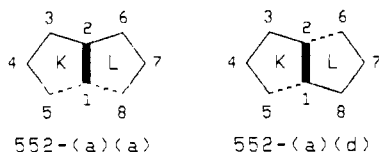
$$t = (2k^2(k-1)/2)/4 = k^2(k-1)/4$$

For the reaction kind $A + X_1 \rightleftharpoons B + X_2$ ($a = 2, b = 2$):

$$\binom{k}{2} = k(k-1)/2 \quad \chi(\gamma_2) = k^2/4 \quad \chi(\gamma_3) = \chi(\gamma_4) = k(k-1)/2$$

$$t = ([k(k-1)/2][k(k-1)/2] + k^2/4 + k(k-1)/2 + k(k-1)/2)/4 = k((k-2)(k^2+6)+8)/16$$

2. Counting the Number of G_3 Graphs. At present we use three vertex labels: C = carbon, N = nitrogen, X = element of main group VI (oxygen, sulfur, or their analogs). The total number of labelings (i.e., G_3 graphs) for three labels and G_1 graphs without symmetry is 3^N , where N is the number of vertices of the G_1 graph. In general, the number of nonequivalent labelings can also be counted by the Cauchy-Frobenius-Burnside lemma, but calculations based on simple sequences from the Polya theorem⁴³ are easier. For example, for the G_1 graph 552-(a)(a) the number of labelings can be counted in the following way.



(1) The automorphism group $\text{Aut}(G_1)$ of this graph consists of two permutations:

$$\Pi = \text{Aut}(G_1) = \{\pi_1, \pi_2\}$$

where $\pi_1 = (1)(2)(3)(4)(5)(6)(7)(8)$ and $\pi_2 = (1)(2)(3,6)(4,7)(5,8)$. (2) Calculate the cycle index for each permutation:

$$Z(\pi_1) = x_1^8 \quad Z(\pi_2) = x_1^2 x_2^3$$

(3) Calculate the cycle index for the group Π :

$$Z(\Pi) = 1/2(x_1^8 + x_1^2 x_2^3)$$

(4) Substitution of $x_i, i = 1, 2$, by the number of labels (3) gives the result:

$$t = 1/2(3^8 + 3^5) = 3402$$

For the G_1 graph 552-(a)(d) the number of labelings can be counted similarly:

$$\Pi = \text{Aut}(G_1) = \{\pi_1, \pi_2\} \quad (1)$$

where $\pi_1 = (1)(2)(3)(4)(5)(6)(7)(8)$ and $\pi_2 = (1,2)(3,8)(4,7)(5,6)$.

$$Z(\pi_1) = x_1^8 \quad Z(\pi_2) = x_2^4 \quad (2)$$

$$Z(\Pi) = 1/2(x_1^8 + x_2^4) \quad (3)$$

$$t = 1/2(3^8 + 3^4) = 3321 \quad (4)$$

Supplementary Material Available: Table of the codes of all possible G_1 graphs which correspond to interconversions of 5-7-membered heterocycles (5 pages). Ordering information is given on any current masthead page.

A diskette with the GREH program for the IBM PC and compatible personal computers is available from Prof. Steve R. Heller, Model and Database Coordination Lab., Agriculture Research Service, BARC-W, Beltsville, MD 20705.

Dynamic Models for the Thermal Deazetization of 2,3-Diazabicyclo[2.2.1]hept-2-ene

Barbara A. Lyons, Jörg Pfeifer, Thomas H. Peterson, and Barry K. Carpenter*

Contribution from the Department of Chemistry, Baker Laboratory, Cornell University, Ithaca, New York 14853-1301. Received September 25, 1992

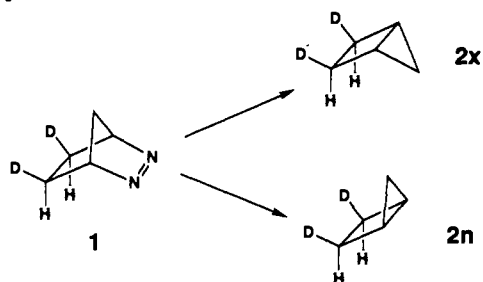
Abstract: Kinetic studies on the thermal nitrogen extrusion from 2,3-diazabicyclo[2.2.1]hept-2-ene-*exo,exo*-5,6-*d*₂ are reported. The ratio of rate constants for formation of the label-isomeric products (bicyclo[2.1.0]pentane-*exo,exo*-2,3-*d*₂ and -*endo,endo*-2,3-*d*₂) is found to exhibit no statistically significant temperature dependence. A comparison of gas-phase and solution-phase results is presented. The results are interpreted in terms of two complementary dynamic models. In the first, classical trajectory calculations are run on a three-dimensional projection (two geometric coordinates) of the potential energy hypersurface. These calculations correctly identify the major product, and reproduce the near temperature-independence of the rate-constant ratio, but do not match the ratio quantitatively. Modification of the trajectory calculations to simulate the effect of collisions with solvent molecules also qualitatively matches the observed difference between gas-phase and solution-phase behavior. In the second model, the vector of atomic displacements corresponding to the reaction coordinate at the transition state for nitrogen loss is identified by both semiempirical and ab initio calculations. The components of this vector pointing along the paths to the post-transition-state minima are computed and are shown to lead to a prediction of the product ratio that is in good (if partly fortuitous) agreement with the experimental result. The vector model is used to predict isotope effects on the product ratio, which are then investigated experimentally with 2,3-diazabicyclo[2.2.1]hept-2-ene-*endo,endo*-1,4,5,6,7,7-*d*₆ and -*endo*-7-*d*.

Introduction

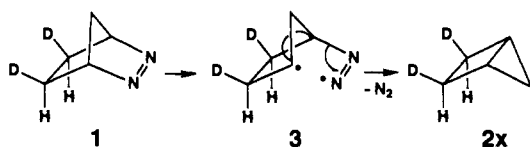
The thermal deazetization of 2,3-diazabicyclo[2.2.1]hept-2-enes has been a source of mechanistic fascination ever since the report by Roth and Martin that the deuterium-labeled parent structure

(compound **1** in Scheme I) underwent the reaction in the gas phase with a preference for inversion of configuration, i.e., giving the *exo*-labeled bicyclo[2.1.0]pentane **2x** in preference to the *endo*-labeled isomer **2n**.¹

Scheme I



Scheme II. The Second of the Roth–Martin Mechanisms for the Title Reaction



Three explanations have been offered for the stereochemistry of the reaction: Roth and Martin initially favored a concerted cleavage of the two C–N bonds of the reactant, with simultaneous C–C bond formation between the back lobes of the carbon-centered orbitals. Later, they proposed that the reaction occurred by stepwise C–N bond cleavage, involving the intermediacy of a diazenyl biradical (3) that underwent loss of nitrogen via an internal S_R2 reaction with inversion of configuration.² This mechanism is illustrated in Scheme II.

Allred and Smith³ observed the inversion of stereochemistry in the deazetization of *exo*- and *endo*-2,3-diaza-5-methoxybicyclo[2.2.1]heptenes and explained it by invoking pyramidalized cyclopentane-1,3-diyl biradicals that were formed with inversion as "... a consequence of recoil from energy released by C–N bond breaking".

The first of the Roth and Martin proposals and the Allred and Smith mechanism (at least in its originally conceived form) can now be ruled out, since there has been convincing recent evidence⁴ that the reaction does, in fact, involve the diazenyl biradical 3, and cannot, therefore, occur with the concerted C–N bond cleavage envisioned in these two mechanisms.

The second Roth and Martin mechanism (Scheme II) provides an explanation for the principal product (2x) but not for the minor product (2n). While it is known that 2x and 2n do thermally interconvert,⁵ the rate of this process is not high enough to explain the amount of 2n observed (*vide infra*). One might consider the possibility that 2x is formed in a chemically activated state, and that its interconversion with 2n would thus be faster than expected for a normal, thermally activated process. Were this explanation correct, the stereoselectivity of the reaction would increase upon changing from gas-phase to solution-phase conditions, since the latter would provide more efficient deactivation of the putative chemically activated 2x. In fact, the stereoselectivity decreases in solution (*vide infra*), and so the chemically activation explanation does not seem viable.

The only explanation for the appearance of 2n that seems consistent with the mechanism of Scheme II is that there exists a competitive pathway that either takes the diazenyl biradical directly to 2n or converts the diazenyl biradical to another intermediate, plausibly cyclopentane-1,3-diyl (structure 4 in Figure 2), that can give both 2x and 2n. Whatever this competitive pathway might be, it seems inevitable that its transition state would have a very different geometry from that implied by the C–C bond

Table I

temp (°C)	time (s)	mole fraction 1	ratio 2x:2n
129.8	41835	0.846	4.22
129.8	86230	0.689	4.63
129.8	128550	0.581	4.86
129.8	172425	0.438	4.56
129.8	257670	0.273	4.24
140.0	14855	0.822	4.94
140.0	29042	0.681	4.40
140.0	58595	0.404	4.36
140.0	85305	0.266	3.69
140.0	134540	0.111	3.32
150.1	7286	0.673	5.04
150.1	14935	0.437	4.13
150.1	22265	0.289	4.37
150.1	36802	0.121	3.67
160.0	3660	0.713	4.57
160.0	7200	0.446	4.74
160.0	10800	0.284	5.03
160.0	14400	0.175	4.46
160.0	18180	0.112	3.88
170.0	1800	0.594	4.12
170.0	3660	0.328	4.40
170.0	5880	0.153	4.40
170.0	7260	0.095	3.90
170.0	9000	0.0298	3.90
180.5	900	0.491	4.74
180.5	1800	0.216	4.31
180.5	2700	0.0677	4.38
180.5	3600	0.0365	3.14

formation and inversion of configuration mandated by the mechanism in Scheme II. Barring coincidence, the difference in geometry between the two transition states should translate to a difference in their energies, and hence a temperature dependence of the ratio of intrinsic rate constants for formation of 2x and 2n from 1. We began our studies of the problem with an investigation of this temperature dependence.

General Kinetic Procedure. Pyrolyses of the deuterium-labeled azo compounds were conducted in sealed Pyrex tubes that had been soaked in 10% aqueous ammonia for 8 h and then oven dried for 4 h. The tubes for the gas-phase experiments contained the azo compound (20 mg for compounds 1 and 4, 6 mg for compound 5) and (in the case of 1) 1,4-dioxane- d_8 (5 μ L) as an internal standard. The tubes for the solution-phase experiments also contained the appropriate solvent (0.65 mL) and benzene- d_6 (6 drops) as a lock for the NMR analysis.

Tubes were immersed in a Tamson silicone oil bath kept at the desired temperature within ± 0.1 °C. Tubes were removed from the bath at timed intervals and then cooled immediately to 0 °C. Tubes for gas-phase experiments were opened, and the contents were dissolved in carbon disulfide containing C_6D_6 . This solution was subjected to 2H NMR spectrometry. Tubes for solution-phase experiments could be analyzed by 2H NMR without opening and could then be returned to the kinetics bath for further reaction.

For compound 4, the inversion:retention ratio in the bicyclo[2.1.0]pentane products was determined from the integral ratio of the signals at δ 1.30 (*endo* deuteriums on C2 and C3) and δ 2.10 (*exo* deuteriums on C2 and C3). Spectra were recorded as an average of eight transients, utilizing a 5 s delay between pulses.

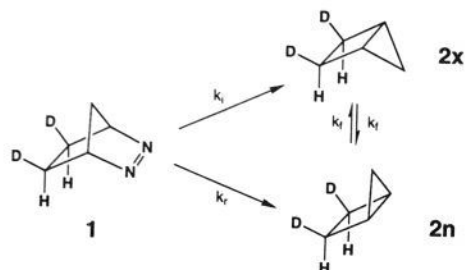
For compound 5, the inversion:retention ratio in the bicyclo[2.1.0]pentane products was determined from the ratio of the integrals of the resonances for the *endo* deuterium on C5 (δ 0.40) and the *exo* deuterium δ 0.56, in the 2H NMR spectrum. The integral ratios were found to be insensitive to pulse delays between 0 and 10 s. Integrations were conducted with 352 transients per spectrum and incorporated no pulse delays.

Kinetic Studies on 2,3-Diazabicyclo[2.2.1]hept-2-ene-*exo*,*exo*-5,6- d_2 . Using the gas-phase procedure described above, the concentration of compound 1 and the ratio of concentrations of label-isomeric products 2x and 2n were measured as a function of both time and temperature, with the results shown in Table I. These data were fit by use of a nonlinear-least-squares routine

(1) Roth, W. R.; Martin, M. *Justus Liebigs Ann. Chem.* 1967, 702, 1.
 (2) Roth, W. R.; Martin, M. *Tetrahedron Lett.* 1967, 4695.
 (3) Allred, E. L.; Smith, R. L. *J. Am. Chem. Soc.* 1967, 89, 7133.
 (4) Simpson, C. J. S. M.; Wilson, G. J.; Adam, W. J. *Am. Chem. Soc.* 1991, 113, 4728. See, also: Adams, J. S.; Burton, K. A.; Andrews, B. K.; Weisman, R. B.; Engel, P. S. *J. Am. Chem. Soc.* 1986, 108, 7935. Adams, J. S.; Weisman, R. B.; Engel, P. S. *J. Am. Chem. Soc.* 1990, 112, 9115.

Table II. Best-Fit Values of the Rate Constants Defined in Scheme III to the Data in Table I

temp (°C)	k_i (s ⁻¹)	k_r (s ⁻¹)	k_f (s ⁻¹)	k_i/k_r
129.8	$(3.81 \pm 0.74) \times 10^{-6}$	$(8.41 \pm 6.41) \times 10^{-7}$	$(3.9 \pm 69.3) \times 10^{-8}$	4.53 ± 2.40
140.0	$(1.25 \pm 0.17) \times 10^{-5}$	$(2.49 \pm 1.59) \times 10^{-6}$	$(1.32 \pm 0.94) \times 10^{-6}$	5.04 ± 2.10
150.1	$(4.66 \pm 0.42) \times 10^{-5}$	$(9.11 \pm 3.97) \times 10^{-6}$	$(3.45 \pm 6.21) \times 10^{-6}$	5.11 ± 1.96
160.0	$(9.42 \pm 1.33) \times 10^{-5}$	$(1.88 \pm 0.56) \times 10^{-5}$	$(3.7 \pm 11.3) \times 10^{-6}$	5.01 ± 2.47
170.0	$(2.53 \pm 0.22) \times 10^{-4}$	$(5.78 \pm 0.37) \times 10^{-5}$	$(4.1 \pm 14.2) \times 10^{-6}$	4.38 ± 1.23
180.5	$(7.19 \pm 1.04) \times 10^{-4}$	$(1.32 \pm 0.83) \times 10^{-4}$	$(4.59 \pm 8.08) \times 10^{-5}$	5.45 ± 3.44

Scheme III. Definition of the Rate Constants for Kinetic Analysis of the Title Reaction

to the following integrated rate equations, describing the overall transformations illustrated in Scheme III.

$$[2x] = 0.5 + \frac{(k_i - k_r) \exp(-2k_f t) + 2(k_f - k_i) \exp(-(k_i + k_r)t)}{2(k_i + k_r - 2k_f)}$$

$$[2n] = 0.5 - \frac{(k_i - k_r) \exp(-2k_f t) + 2(k_f - k_i) \exp(-(k_i + k_r)t)}{2(k_i + k_r - 2k_f)}$$

$$[1] = 1 - [2x] - [2n]$$

Scheme III serves to define the gross rate constants used in the integrated rate equations. It does not imply anything about a detailed mechanism.

The best-fit rate constants are summarized in Table II.

The large errors in the best-fit values of k_r reflect the relative insensitivity of the results to this parameter. The interconversion of **2x** and **2n** during the kinetics experiment, especially at the lower temperatures, did not cause changes in their relative concentration that were outside of our experimental error.

The substantial uncertainties (reported for the 95% confidence interval) propagated into the k_i/k_r ratio required that the question of temperature dependence be addressed by careful statistical analysis.⁶ This was accomplished as follows.

First, the sum of squares due to purely experimental error (SS_{pe}) was calculated from the formula

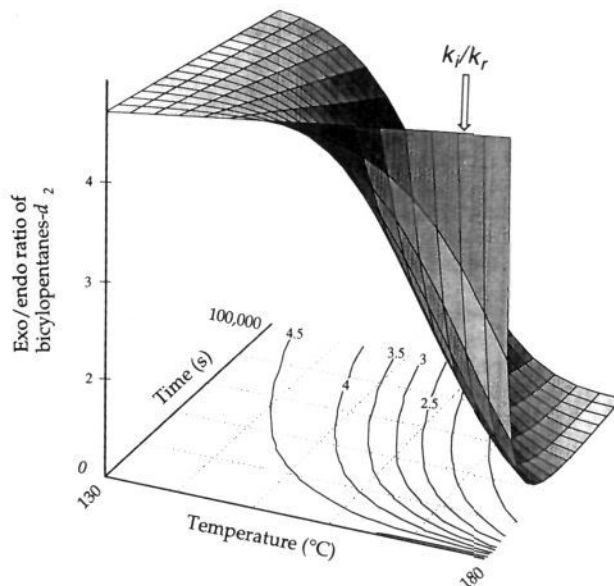
$$SS_{pe} = \sum_T \sum_t (R_{Tt} - \bar{R}_{Tt})^2 = 1.60441$$

where R_{Tt} is the observed ratio of **2x:2n** at each temperature and time (reported in Table I) and \bar{R}_{Tt} is the ratio of **2x:2n** calculated from the best-fit k_i/k_r ratio at each temperature (from Table II). The subscripts on the various ratios serve to specify the factors that can influence their value, T being temperature and t being time.

Next, the sum of squares of the residuals for a temperature-independent model ($SS_r(T_{ind})$) was calculated from the formula

$$SS_r(T_{ind}) = \sum_T \sum_t (R_{Tt} - \bar{R}_t)^2 = 2.25056$$

where \bar{R}_t is the **2x:2n** ratio calculated using the weighted average

**Figure 1.** Best-fit form of the integrated rate equations and relative activation parameters for conversion of **1** to **2x** and **2n**.

of best-fit k_i/k_r values ($=4.74$).

The sum of squares of the residuals for a temperature-dependent model ($SS_r(T_{dep})$) was calculated from the formula

$$SS_r(T_{dep}) = \sum_T \sum_t (R_{Tt} - \hat{R}_{Tt})^2 = 2.16538$$

where \hat{R}_{Tt} is the **2x:2n** ratio computed using values for k_i/k_r calculated from the formula

$$\frac{k_i}{k_r} = \exp\left(\frac{-\Delta\Delta H^\ddagger}{RT}\right) \exp\left(\frac{\Delta\Delta S^\ddagger}{R}\right)$$

Here $\Delta\Delta H^\ddagger$ and $\Delta\Delta S^\ddagger$ are the differences in activation enthalpy and entropy (for the reactions giving **2x** and **2n**) that best fit the observed \hat{R}_T . The values of the relative activation parameters turned out to be highly dependent on the statistical model used to fit the data. An unweighted nonlinear least-squares fit gave values of $\Delta\Delta H^\ddagger = 540 \pm 860$ cal/mol and $\Delta\Delta S^\ddagger = 4.4 \pm 1.8$ cal/(mol K), whereas a nonlinear least-squares fit, in which the \hat{R}_T values were given statistical weights equal to the reciprocal of their variances, gave $\Delta\Delta H^\ddagger = -470 \pm 900$ cal/mol and $\Delta\Delta S^\ddagger = 2.0 \pm 1.9$ cal/(mol K). The former values were used for the specific calculations cited below, although the final conclusion was the same with either set (vide infra).

The sums of squares due to lack of fit of each model ($SS_{lof}(T_{ind})$ and $SS_{lof}(T_{dep})$) were derived by simple subtraction.

$$SS_{lof}(T_{ind}) = SS_r(T_{ind}) - SS_{pe} = 0.64615$$

$$SS_{lof}(T_{dep}) = SS_r(T_{dep}) - SS_{pe} = 0.56097$$

The variance due to lack of fit of each model ($s_{lof}^2(T_{ind})$ and $s_{lof}^2(T_{dep})$) could then be calculated by dividing by the number of degrees of freedom (four for the temperature-independent model and three for the temperature-dependent model).

(5) Baldwin, J. E.; Ollerenshaw, J. J. *Org. Chem.* **1981**, *46*, 2116.

(6) Deming, S. N. *Experimental Design: a Chemometric Approach*; Elsevier: Amsterdam, 1987.

$$s_{\text{lor}}^2(T_{\text{ind}}) = SS_{\text{lor}}(T_{\text{ind}})/4 \\ = 0.16154$$

$$s_{\text{lor}}^2(T_{\text{dep}}) = SS_{\text{lor}}(T_{\text{dep}})/3 \\ = 0.18699$$

Had the variance of the temperature-dependent model been greater than that of the temperature-independent model, one could have used their ratio in a Fisher *F* test in order to determine the statistical significance of the temperature dependence.⁷ However, since the ratio turned out to be less than unity (0.864), one could conclude that there was no statistically significant temperature dependence of the k_i/k_r ratio. The ratio of variances for the two models was calculated to be 0.850 when the relative activation parameters from the weighted nonlinear least-squares fit were used in the temperature-dependent model.⁸

The best-fit function for the data in Table I is illustrated graphically in Figure 1. At the limit where time approaches zero, the value of the $2x:2n$ ratio should be equal to the k_i/k_r ratio, and in this region the function can be seen to be effectively independent of temperature.

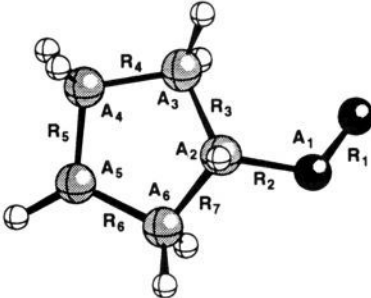
The lack of significant temperature dependence on the k_i/k_r ratio could perhaps have been explained as a coincidental equality of activation enthalpy for the two putative reactions giving **2x** and **2n** from **1**, but we were reluctant to invoke such a coincidence. We had reported similar behavior in three other reactions⁹ and found the coincidental-equality explanation even more unlikely when the results were viewed as a whole.

Alternative explanations for the stereochemistry of the deazetization of compound **1**, and the experiments designed to test them, form the basis of the remainder of this paper.

Trajectory Calculations on a Limited-Dimensional Projection of the Potential-Energy Surface. Since the stereochemistry of the title reaction could be set only at the time of cleavage of the second C–N bond (i.e., the remaining C–N bond of the diazenyl biradical), this was the region of the potential energy surface that we chose to explore.

An enthalpy surface for the reaction was created from a combination of experimental heats of formation, Benson group-additivity calculations, and AM1 semiempirical molecular orbital calculations.¹⁰ The reason for using this mixed-mode estimation method was that the AM1 calculations, using the minimal CI necessary for proper description of a singlet biradical,¹¹ did a very poor job in evaluating the enthalpy difference between bicyclo[2.1.0]pentane and cyclopentane-1,3-diyl. According to Benson group additivity (as amended by the Doering correction¹²), the biradical should have a heat of formation of 71.3 kcal/mol, placing it 34.0 kcal/mol above the bicyclic structure.¹³ This result is in good agreement with the experimental heat of formation of 71.5 ± 2.3 kcal/mol for cyclopentane-1,3-diyl.¹⁴ In combination with

Table III. Comparison of Semiempirical and ab Initio Geometries and Relative Energies for the Diazenyl Biradical and Its Transition State for Nitrogen Loss



	AM1-CI (Singlet)		AM1-UHF (Triplet)		UHF/6-31G* (Triplet)	
	AM1-CI (singlet)		AM1-UHF (triplet)		UHF/6-31G* (triplet)	
	biradical	TS	biradical	TS	biradical	TS
R_1	1.150	1.119	1.151	1.121	1.173	1.133
R_2	1.467	1.870	1.469	1.844	1.491	1.792
R_3	1.547	1.506	1.545	1.507	1.532	1.521
R_4	1.527	1.534	1.528	1.533	1.539	1.543
R_5	1.468	1.475	1.472	1.475	1.507	1.506
R_6	1.473	1.480	1.471	1.477	1.503	1.506
R_7	1.550	1.510	1.547	1.509	1.536	1.524
A_1	138.4	129.7	138.0	129.6	120.3	116.3
A_2	106.7	109.6	106.5	109.0	105.0	107.2
A_3	106.6	106.5	106.6	106.6	103.4	103.8
A_4	106.9	106.4	106.6	106.1	103.5	103.6
A_5	112.7	111.9	112.6	112.0	111.5	111.7
A_6	105.7	105.5	105.7	105.6	102.5	102.9
$\langle S^2 \rangle$			2.023	2.043	2.130	2.156
E_{rel} [0]		14.9 ^a	[0]	13.0 ^a	[0]	6.3 ^b

^a Enthalpy difference. ^b Potential energy difference, uncorrected for zero-point energies.

the experimental activation enthalpy of 36.9 kcal/mol for the stereochemical inversion of bicyclo[2.1.0]pentane-*exo,exo*-2,3- d_2 ,⁵ it suggests a barrier of about 1–3 kcal/mol for closure of cyclopentane-1,3-diyl to bicyclo[2.1.0]pentane. This estimate is in accord with the conclusion from ab initio calculations that singlet cyclopentane-1,3-diyl has a barrier of about 1 kcal/mol to ring closure.¹⁵

AM1-CI, by contrast, places singlet cyclopentane-1,3-diyl 9.7 kcal/mol below bicyclo[2.1.0]pentane. One might guess that this error arises because of the effective double correction for electron correlation that occurs when CI is performed in a semiempirical scheme that is supposed to be parameterized to include electron correlation with single-determinant wave functions. Arguing against such an interpretation is the fact that an AM1-UHF calculation on the lowest triplet state of cyclopentane-1,3-diyl placed it 17.7 kcal/mol below bicyclo[2.1.0]pentane. Since the singlet–triplet gap in cyclopentane-1,3-diyl is believed to be very small, a calculation on the triplet should also have given a reasonable estimate of the energy of the singlet, but without the potential problem due to the CI. It is not obvious why the observed outcome was so different from this expectation. (The problem was not caused by significant spin contamination in the UHF wave function since $\langle S^2 \rangle = 2.0274$.) In any event, it was clear that the AM1 procedure alone could not be trusted to give a complete enthalpy surface for the reaction of interest.

Presumably ab initio calculations at a high enough level could have given a reliable surface for the reaction, but the considerable expenditure of computer time required for ab initio calculations on singlet biradicals¹⁶ did not seem to make exploration of a complete surface by such methods feasible. We elected, therefore,

(7) Miller, J. C.; Miller, J. N. *Statistics for Analytical Chemistry*, 2nd ed.; Ellis Horwood Ltd.: Chichester, 1988.

(8) In our original communication on this work (Lyons, B. A.; Pfeifer, J.; Carpenter, B. K. *J. Am. Chem. Soc.* **1991**, *113*, 9006) an *F* test on the ratio of total variances was used (footnote 4 in the communication). While the conclusions were the same as here, we now think that an *F* test on the ratio of variances due to lack of fit of each model is a better way of assessing the issue of temperature dependence, since it is less susceptible to spurious agreements with the null hypothesis, which can arise when there is large purely experimental error.

(9) Newman-Evans, R. H.; Simon, R. J.; Carpenter, B. K. *J. Org. Chem.* **1990**, *55*, 695.

(10) (a) Experimental heat of formation for bicyclo[2.1.0]pentane: Turner, B. B.; Goebel, P.; Mallon, B. J.; Doering, W. von E.; Coburn, J. F.; Pomerantz, M. *J. Am. Chem. Soc.* **1968**, *90*, 4315. (b) AM1 calculation: Dewar, M. J. S.; Zoebisch, E. G.; Healy, E. F.; Stewart, J. J. P. *J. Am. Chem. Soc.* **1985**, *107*, 3902. See, also: refs 13–15 and 17.

(11) Salem, L.; Rowland, C. *Angew. Chem., Int. Ed. Engl.* **1972**, *11*, 92.

(12) Doering, W. von E. *Proc. Natl. Acad. Sci. U.S.A.* **1981**, *78*, 5279.

(13) Benson, S. W. *Thermochemical Kinetics*, 2nd ed.; Wiley-Interscience: New York, 1976. There may be hazards associated with using Benson group additivity to estimate heats of formation of biradicals with large singlet–triplet energy gaps. Fortunately, theoretical work on cyclopentane-1,3-diyl suggests a gap of only ~ 1 kcal/mol (ref 15).

(14) Goodman, J. L.; Herman, M. S. *J. Am. Chem. Soc.* **1988**, *110*, 2681.

(15) Sherrill, C. D.; Seidl, E. T.; Schaefer, H. F., III *J. Phys. Chem.* **1992**, *96*, 3712.

(16) For a recent example, see: Getty, S. J.; Davidson, E. R.; Borden, W. T. *J. Am. Chem. Soc.* **1992**, *104*, 2085.

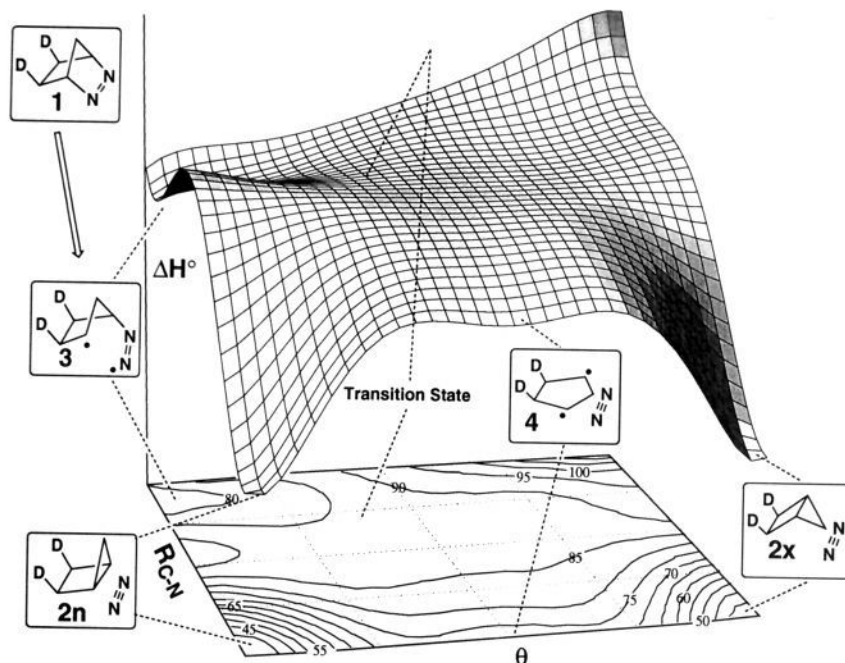


Figure 2. Semiempirical enthalpy surface for the title reaction. See text for definitions of R_{C-N} and θ .

to use the experimental and Benson group-additivity values for heats of formation to provide anchors for all stationary points except the transition state for loss of nitrogen from the diazenyl biradical (where no such values were available). It seemed plausible that the geometry and relative energy of this transition state could be described reasonably well by the AM1 procedure, because the method seemed to get the enthalpy of reaction for conversion of the diazenyl biradical to cyclopentane-1,3-diyl plus nitrogen just about right (-12.2 kcal/mol for the singlet and -13.7 for the triplet, compared to an estimated reaction enthalpy less negative than -14.3 , according to a combination of experimental observations and Benson group additivity calculations¹⁷).

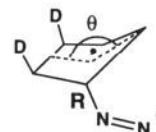
The computed activation barrier and transition-state geometry for the triplet reaction were compared with those from an ab initio UHF/6-31G* calculation.¹⁸ A comparison was also made between singlet and triplet biradicals with the AM1 method. The results are given in Table III. The results from the ab initio calculation are somewhat different from the AM1-UHF calculation, most notably in the lower activation barrier to nitrogen loss. It is not clear that ab initio results are more reliable, however, since the overall enthalpy of reaction calculated with a UHF/6-31G* wave function is -24.3 kcal/mol, which deviates more from the Benson value than the AM1 number does.

Perhaps in accord with one's intuition, the singlet and triplet diazenyl biradicals are calculated to have very similar structures

and very similar activation enthalpies for nitrogen loss, according to AM1.

Overall, while there were some concerns about the use of the AM1 procedure for this problem, it appeared that it would give at least a semiquantitative description of the potential energy surface in the vicinity of the transition state for nitrogen loss from the diazenyl biradical.

Structures on the singlet surface of the diazenyl biradical were calculated with various values of R , the C-N bond distance, and θ , the angle between the planes defined by C1-C7-C4 and the average plane of C1-C5-C6-C4 (in bicyclo[2.1.0]pentane, θ represents the angle between the planes of the three- and four-membered rings), with all other geometrical parameters allowed to adopt their lowest energy values. A polynomial with terms up to $\theta^6 R^4$ was fit to these points by a least-squares procedure. This



piece of the surface was then translated along the enthalpy axis until it joined the surface where experimental points were available—i.e., in the region of cyclopentane-1,3-diyl and bicyclo[2.1.0]pentane. A single polynomial that represented a best fit to all of the points was then calculated. The resulting surface is shown in Figure 2. For the purposes of the following dynamics calculations, the relative enthalpies of the species on this surface were assumed to be equal to their relative potential energies.

Classical trajectory calculations were run on the surface as follows. The trajectories were started from a plane perpendicular to the reaction coordinate, just 0.2 kcal/mol below the transition state. This device permitted attention to be focussed on just those molecules having enough internal energy to cross the barrier to reaction after a single collision. Trajectories were calculated for molecules with initial kinetic energies that varied from 0.0 to 2.0 kcal/mol in 0.1 kcal/mol increments, and geometries that corresponded to 67 different locations along the starting plane. Initial directions were varied through 360° in 10° increments. The resulting $50\,652$ trajectories were tracked until they reached one of the four minima on the surface (the two bicyclopentane epimers, the starting diazenyl biradical or cyclopentane-1,3-diyl).

Calculation of a single trajectory involved the following steps. From the initial position, direction, and kinetic energy selected

(17) The Benson-group method, using a Doering correction of 5.4 kcal/mol and a ring strain of 5.9 kcal/mol gives $\Delta H_f^\circ = 71.3$ kcal/mol for cyclopentane-1,3-diyl. The experimental heat of formation for 2,3-diazabicyclo[2.2.1]hept-2-ene is 49.6 kcal/mol, and the activation enthalpy for its deazetization is 36.0 kcal/mol (Engel, P. S. *Chem. Rev.* **1980**, *80*, 99), giving a heat of formation of the rate-limiting transition state of 85.6 kcal/mol. Since the reaction does apparently involve the diazenyl biradical as an intermediate, its heat of formation must presumably be <85.6 kcal/mol, making the enthalpy of its conversion to cyclopentane-1,3-diyl >-14.3 kcal/mol. A direct calculation of the heat of formation of the diazenyl biradical using a Doering correction of 2.7 kcal/mol and a ring strain of 6.1 kcal/mol, with Engel's values for the azo radical group contributions (Engel, P. S.; Wood, J. L.; Sweet, J. A.; Margrave, J. L. *J. Am. Chem. Soc.* **1974**, *96*, 2381) gives a value of 88.3 kcal/mol, which is apparently somewhat too high. Perhaps the singlet-triplet energy gap in the diazenyl biradical is larger than in cyclopentane-1,3-diyl, in which case the direct estimate of the heat of formation of the former by Benson group additivity would be unreliable.

(18) Ab initio calculations used the Gaussian 88 package (Gaussian 88, Frisch, M. J.; Head-Gordon, M.; Schlegel, H. B.; Raghavachari, K.; Binkley, J. S.; Gonzalez, C.; Defrees, D. J.; Fox, D. J.; Whiteside, R. A.; Seeger, R.; Melius, C. F.; Baker, J.; Martin, R. L.; Kahn, L. R.; Stewart, J. J. P.; Fluder, E. M.; Topiol, S.; Pople, J. A. Gaussian, Inc.: Pittsburgh, PA).

as described above, a velocity for straight-line motion (in mass-weighted coordinates) could be computed from Newton's Laws of Motion—the "motion" being of a point that summarizes the values of the parameters R and θ . After a short straight-line segment (see below for a description of the procedure used in selecting step lengths), the potential energy function was differentiated with respect to R and θ in order to determine the new forces acting on the atoms. These forces were used to amend the magnitude and direction of the velocity for the next segment. The curved reaction trajectory was thus constructed from small straight-line segments. The lengths of these segments were adjustable. A calculation with a given segment length was checked for conservation of total (kinetic plus potential) energy. If it passed within the selected tolerance (0.01 kcal/mol for the entire trajectory and 10^{-5} kcal/mol per segment) the segment length was doubled for the next step. If the segment failed the energy-conservation test, it was recomputed with a step of half the length. This reduction in step length was repeated until the test was passed. The need for many thousands of potential energy derivatives made the use of a polynomial form for the potential function computationally efficient.

Since the trajectories were not tracked after entering a minimum, the results correspond in experimental terms to the determined ratios of k_i/k_r , rather than to the $[2x]/[2n]$ ratios that were actually measured. The reactive trajectories were counted as follows. Each trajectory was given a statistical weight corresponding to the product of Boltzmann factors for its starting potential and kinetic energy at the temperature of interest. Trajectories leading to cyclopentane-1,3-diyl were assumed to lead eventually to one of the stereoisomeric bicyclo[2.1.0]pentanes, with a probability of 0.5. The calculations were run for six different temperatures in 10° increments between 130 and 180 $^\circ\text{C}$.

The results were that k_i/k_r was computed to vary between 2.30 at 130 $^\circ\text{C}$ and 2.22 at 180 $^\circ\text{C}$. Thus, the preference for inversion of stereochemistry was correctly identified, as was the near temperature independence of the rate constant ratio. The magnitude of this ratio (experimentally 4.7) was not correctly reproduced, although that is perhaps not surprising given the uncertainties about the potential energy surface.

Of particular interest was the *reason* that the trajectory calculations correctly described the overall stereochemical preference of the reaction. The answer was readily seen when some representative trajectories were plotted out on a contour map of the surface. The results are shown in Figure 3. For the purpose of comparison, three trajectories starting from the same point are shown; they differ only in the direction of their initial motion. One can see that trajectory *a* had too large a fraction of its initial kinetic energy in the R direction and hence was unable to cross the barrier to nitrogen loss. Trajectory *c* had too large a fraction in the θ direction and was similarly reflected back to the bound diazenyl biradical. Trajectory *b* had a ratio of R and θ motions that was within the relatively narrow window permitting reaction. The reaction coordinate from the diazenyl biradical to the transition state for its loss of nitrogen involves changes in both the R and θ parameters; this combination of R and θ displacements both defines the reactive trajectory *b* and, by conservation of momentum, mandates its continuation toward the inversion product. In more picturesque language, one can say that *there is a "beam" of trajectories that has the correct combination of R and θ motions to permit loss of nitrogen, and this beam is pointing roughly in the direction of the inversion product*. The retention product can be formed by trajectories starting from other points on the surface, or trajectories with higher initial kinetic energy, but in general the preference for formation of the inversion product persists for the reason cited.

Theoretical Simulation and Experimental Determination of Medium Effects on the Reaction Stereochemistry. As a test of the computational model described above, we sought to simulate the effect of changing the reaction medium from gas phase to solution phase. In the trajectory calculations the effect of solvent-solute interactions was simulated by the following rather crude device. Pseudocollisions were introduced with the following

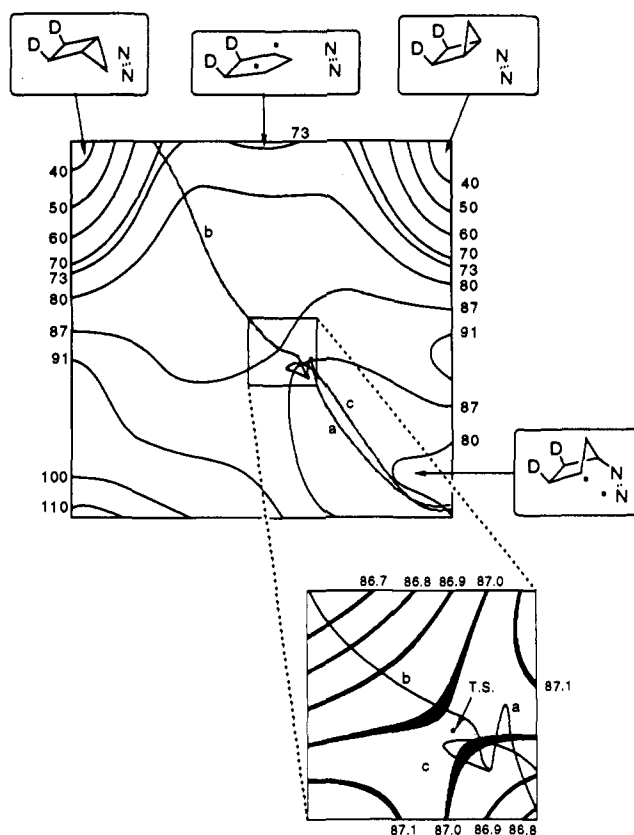


Figure 3. Trajectories for the title reaction superimposed on a contour plot of the surface in Figure 2. For the purposes of comparison the three illustrated trajectories were started from a point on the reaction coordinate and 0.2 kcal/mol below the transition state. The initial conditions differed only in the direction of the trajectories.

properties: (1) The duration of each collision was infinitely short (and hence physically unrealistic). (2) The average frequency of collisions was selectable as a reaction parameter. The distribution of frequencies about the chosen average was set by the selected temperature (only 150 $^\circ\text{C}$ was investigated). (3) The effect of each collision was to cause a random change in direction of a reaction trajectory. (4) The kinetic energies of the reacting molecule and its collision partner were adjusted in the direction of the average of the two but with an upper limit of 2 kcal/mol change per collision. The effect of these "collisions" was thus usually to "cool" reacting molecules when they were over low potential energy parts of the surface but sometimes to energize reacting molecules that were in high potential energy regions (where conservation of energy would require that their kinetic energy was low and therefore likely to be increased by collision). The k_i/k_r ratio was determined as a function of the average frequency of the collisions. The result is depicted in Figure 4. The curve in Figure 4 is for purposes of illustration only—it has no theoretical significance.

The conclusions from the calculations were that collisions with molecules constituting the surrounding medium would be expected to reduce the magnitude of k_i/k_r , but that the effective collision frequency required to completely wash out the dynamic effect would be higher than one could achieve even in solution.¹⁹ Accordingly, we set out to investigate the reaction in solution experimentally.

The deazetization reaction was examined at a variety of temperatures in three different solvents: *trans*-decalin, *cis*-decalin, and dibenzyl ether. The best-fit k_i/k_r ratios were determined as described earlier. The results are summarized in Table IV.

As can be seen, the expectation that k_i/k_r should approach but not reach unity was borne out in all three solvents. The uncer-

(19) Chandler, D. *J. Stat. Phys.* 1986, 42, 49.

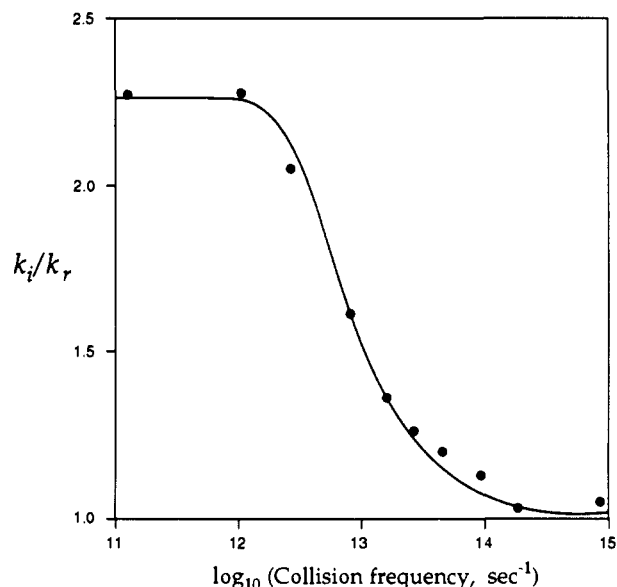


Figure 4. Predicted dependence of k_i/k_r on frequency of collisions with molecules in the surrounding medium.

Table IV

<i>trans</i> -decalin		<i>cis</i> -decalin		dibenzyl ether	
T (°C)	k_i/k_r	T (°C)	k_i/k_r	T (°C)	k_i/k_r
129.7	1.96 ± 0.10	129.7	1.73 ± 0.13	130.8	1.69 ± 0.07
140.2	2.05 ± 0.06	140.2	1.79 ± 0.05	140.0	1.77 ± 0.14
149.8	2.12 ± 0.11	150.3	1.70 ± 0.12	150.5	1.61 ± 0.37
161.8	2.06 ± 0.09	161.8	1.88 ± 0.07	159.8	1.66 ± 0.06
170.5	2.03 ± 0.09	170.5	1.80 ± 0.12	170.1	1.77 ± 0.34
186.5	2.22 ± 0.22	180.3	1.76 ± 0.13	176.0	1.76 ± 0.13
				182.5	1.71 ± 0.28

tainties in the best-fit rate-constant ratios were much smaller than for the gas-phase studies, presumably because it was no longer necessary to use a separate kinetics tube for every point—the reaction could be run in a NMR tube which could be quenched, analyzed, and then returned to the bath.

Once again, there was no statistically significant temperature dependence to the ratio k_i/k_r . There was, however, statistically significant dependence of the ratio on the nature of the solvent. A one-way analysis-of-variance (ANOVA) test⁷ showed that the weighted mean values for k_i/k_r were dependent on the choice of solvent, with better than 99% confidence.

The reasons for the dependence of the rate-constant ratio on the nature of the solvent are undoubtedly complex, but one intriguing possibility is suggested by the difference between the values in *trans*- and *cis*-decalin (this difference is significant at the 97% level). This pair of solvents was chosen because, while their bulk physical properties would be expected to be similar, their molecular characteristics are different—the *trans* isomer being a more rigid molecule than the *cis*. In theories of intermolecular energy exchange in polyatomic liquids, an important role is assigned to V-V mechanisms, i.e., energy exchange between vibrational modes of one molecule and another.²⁰ The facility of such exchange at low levels of energization would be expected to be greatest when the density of vibrational state is highest. A high density of vibrational states at low energies defines a molecule with a large number of low-frequency vibrational modes—a description that better fits the flexible *cis*-decalin than the more rigid *trans*-decalin. We had anticipated, therefore, that the k_i/k_r ratio might be somewhat closer to unity in the *cis*-decalin. The fact that it turned out that way does not mean that the reason was correctly identified, of course. The observation that the rate-constant ratio is lowest in dibenzyl ether would fit the picture,

because this solvent has internal rotations that would have very high-state densities at low energy. On the other hand, there are obviously large differences in bulk properties between dibenzyl ether and the decalins, and so there can be no clear identification of a single responsible factor for the solvent effect in these experiments.

A clearer dissection of important factors should be possible by studying the reaction in supercritical fluids at various pressures.²¹ Experiments of this kind are planned.

Vectorial Decomposition of the Reaction Coordinate.²² A critical point on the potential energy surface for decomposition of diazenyl biradical **3** was obviously the transition state for cleavage of the remaining C-N bond. As described above, molecular orbital calculations were carried out on this transition state. The vibrational analyses that were part of these computations revealed, as required,²³ a single imaginary frequency. The atomic motions corresponding to the imaginary frequency define the reaction coordinate, as illustrated in Figure 5 for an AM1-CI calculation on the singlet state. The UHF/6-31G* calculations on the triplet yielded a picture that looked virtually identical.

A striking feature of the reaction coordinate was the conformational change occurring in the hydrocarbon fragment as the nitrogen departed. According to the calculations, the reaction coordinate for nitrogen expulsion "imprinted" on the hydrocarbon fragment a set of atomic motions that carried it to a part of the potential energy hypersurface where the arrangement of atoms was closer to the structure of **2x** than **2n**. For the triplet state, which would require a spin change before product formation could occur, such dynamic events may be of little consequence, but for the singlet biradical, which could presumably collapse to products very rapidly, the dynamics might provide an explanation for the experimentally observed preference for formation of **2x** over **2n**. This picture is really a restatement of the results from the previous trajectory calculations.

The pictorial representation of the reaction dynamics could be translated into a semiquantitative prediction of the k_i/k_r ratio. The Cartesian atomic displacements corresponding to the reaction coordinate represent the elements of a $3N$ -dimensional vector (where N is the number of atoms). This vector can be thought of as the center of the beam of reactive trajectories described earlier, except that the full-dimensional space of the problem has now been used. We hypothesized that the product ratio could be estimated by comparing components of the mass-weighted reaction-coordinate vector along directions leading to post-transition-state minima on the potential energy hypersurface.

Before this hypothesis could be tested, certain technical problems had to be overcome. First, it was necessary to define rigorously the "direction" from the transition state to the various post-transition-state minima. A first approximation could be conceived to be the vector derived by simple subtraction of the x , y , and z coordinates of the atoms of the transition state from those of the corresponding atoms in the post-transition-state structure of interest. In order for the calculation to be physically meaningful, however, it was necessary that the transformation defined by such a vector be one that conserved translational momentum and rotational angular momentum. The conservation of translational momentum was easily assured by placing the center of mass of each structure at the origin of the Cartesian coordinate system. Enforcement of conservation of rotational angular momentum was assured by orienting the two structures in such a way that the function

$$\sum_i^N m_i((x_{i1} - x_{i2})^2 + (y_{i1} - y_{i2})^2 + (z_{i1} - z_{i2})^2)$$

(m_i = mass of atom i , x_{ij} = x coordinate of atom i in structure j , etc) was minimized.²⁴ The anchoring of the origins and or-

(20) Oxtoby, D. W. *Adv. Chem. Phys.* **1981**, *47* (part 2), 487 and references therein.

(21) (a) Johnston, K. P. In *Supercritical Fluid Science and Technology*; Penninger, J. M. L., Ed.; ACS Symposium Series: 1989, pp 1-12. (b) Troe, J. J. *Phys. Chem.* **1986**, *90*, 357.

(22) Peterson, T. H.; Carpenter, B. K. *J. Am. Chem. Soc.* **1992**, *114*, 766.

(23) Stanton, R. E.; Melver, J. W., Jr. *J. Am. Chem. Soc.* **1975**, *97*, 3632.

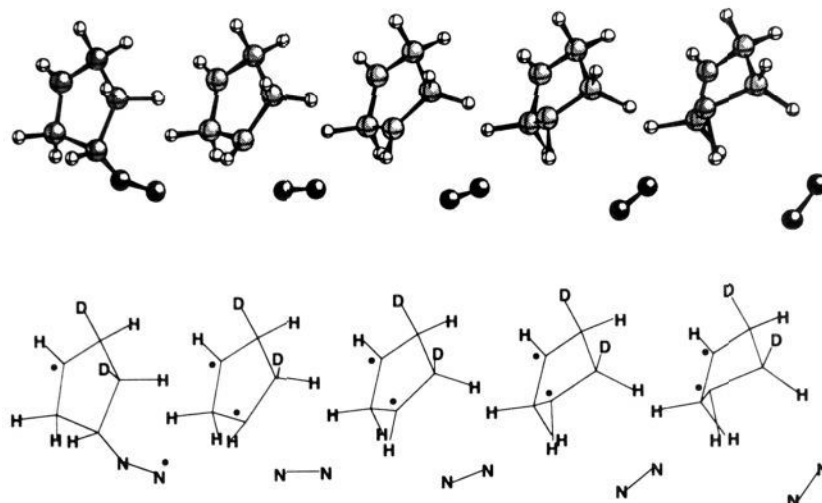


Figure 5. Reaction coordinate for nitrogen loss from the diazenyl biradical, from AM1-CI calculations on the lowest singlet state.

tational orientations of the post-transition-state structures served to reduce the effective dimensions of the problem from $3N$ to the expected $3N-6$.

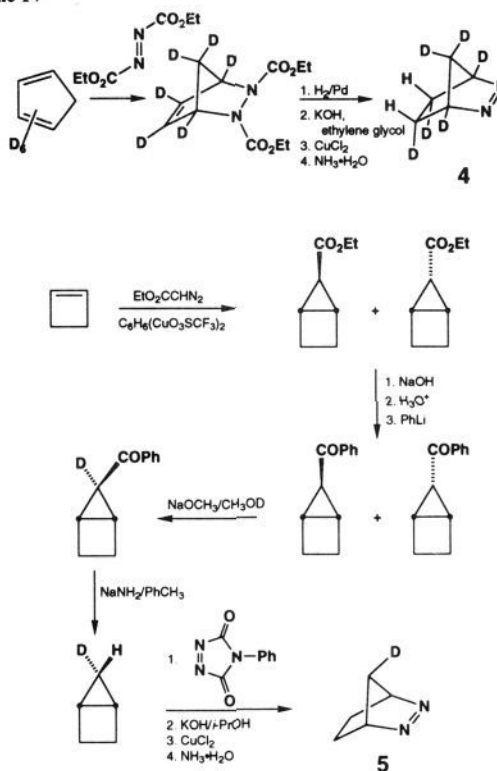
The second technical problem was associated with path curvature. Even when the translational and angular momentum issues had been resolved, the transformation vectors defined above could not be viewed as realistic descriptions of the atomic motions that would convert the transition structure into the structures at the post-transition-state minima. The vectors described a linear synchronous motion in which each atom would move a distance that stayed in a fixed ratio to the motions of the other atoms. This kind of restriction is physically unrealistic if the geometry changes involved are large. In reality, certain atoms will move more at the beginning of the transformation and less at the end. This asynchronous behavior corresponds to curvature of the transformation vector in the $3N-6$ dimensional space. In order to accommodate such path curvature, the following procedure was adopted. A short step (vide infra) in the direction defined by one of the zeroth-order transformation vectors was taken. This structure was then reoptimized (in $3N-5$ dimensions—a single constraint being used to prevent collapse to a stationary point) using the geometry-optimizer of the molecular orbital program. This procedure served to locate a structure on the true (within the limits of the quantum-mechanical model) curved path between transition state and product. A transformation vector from the transition state to this new point was then computed as described above.

The length of the original "short step" was not critical within certain limits. If the step were too short, the "noise" in the geometry optimizer would give unreliable results. If it were too long, the reoptimized structure would be too far away from the transition state for its formation to be reasonably approximated by a linear-synchronous-transit vector. Experience revealed that a suitable compromise occurred with step lengths corresponding to about 30% of the original vector. Between 20 and 40% there was little difference in the final computed results. These figures are presumably specific to the particular reaction and not necessarily generally applicable.

Once the final transformation vectors had been computed from the transition state to each of the post-transition-state minima, they were normalized and then their dot products with the reaction-coordinate vector computed. The ratio of dot products was used to estimate the product ratio.

The results from the AM1-CI calculations were as follows: for azo compound **1** the calculated k_i/k_r ratio was 4.3 (the observed value is 4.7 ± 0.9). This level of agreement could be shown to be partly fortuitous, because for 2,3-diazabicyclo[2.1.1]hex-2-

Scheme IV



ene-*exo*-5- d^{25} the calculated value was 1.9, whereas the observed value is 1.2. If the transition-state geometry and reaction-coordinate vector from the UHF/6-31G* calculations on the triplet state of **3** (in combination with UHF/6-31G* calculations on triplet cyclopentane-1,3-diy and RHF/6-31G* calculations on singlet bicyclo[2.1.0]pentane) were taken as approximations to those that would have been obtained for the singlet states, then the computed k_i/k_r ratio for **1** was 3.7, suggesting relative insensitivity of the results to the nature of the quantum-mechanical model.

Theoretical Prediction and Experimental Determination of Isotope Effects on the k_i/k_r Ratio. It seemed that a useful test of the model would be to predict and then measure isotope effects on the product ratio for 2,3-diazabicyclo[2.2.1]hept-2-ene. The hope was that there would be a tendency for cancellation of errors, because the same potential energy surface would be used in each

(24) (a) Natanzon, G. A.; Adamov, M. *Vestn. Leningrad. Univ., Fiz. Khim.* 1974, 4, 24. (b) Jorgensen, F. *Int. J. Quant. Chem.* 1978, 14, 55.

(25) Chang, M. H.; Dougherty, D. A. *J. Am. Chem. Soc.* 1982, 104, 1131.

case. Only the masses of the atoms, and hence the directions of the reaction-coordinate and transformation vectors, would be changed.

Accordingly we prepared 2,3-diazabicyclo[2.2.1]hept-2-ene-endo-endo-1,4,5,6,7,7- d_6 (**4**) and 2,3-diazabicyclo[2.2.1]hept-2-ene-endo-7- d (**5**), as shown in Scheme IV. For **4**, the calculated isotope effect on k_i/k_r (d_1/d_2) was 1.099, and the measured value was 1.10 ± 0.04 (95% confidence interval for four measurements). The calculated and observed ratios (d_1/d_2) for **5** were 0.936 and 0.93 ± 0.04 . One can see that, although the best estimates of the isotope effects were close to the predicted values, the wide experimental error bars did not permit the results to be viewed as providing unambiguous support for the model.

Conclusion

While no single experimental or theoretical result in this study can be considered to constitute unassailable support for a dynamic explanation of the preferred inversion of stereochemistry in the title reaction, we believe that the following observations, taken in total, are best accommodated by such a picture: (1) the lack of statistically significant temperature dependence on the k_i/k_r ratio, (2) the semiquantitative agreement between the trajectory calculations and the experimental result, including correct identification of the major product and simulation of the near temperature independence of the k_i/k_r ratio, (3) the decrease in k_i/k_r that accompanies transfer from the gas phase to solution (while still maintaining apparent temperature independence), (4) the conformational change seen in both semiempirical and ab initio calculations on the reaction coordinate for loss of nitrogen from **3**, (5) the semiquantitative agreement between the predictions of the vector-resolution model and the experimental result, and (6) the agreement, within rather wide error limits, between the calculated and observed isotope effects on k_i/k_r .

The mechanism that we have described is quite similar to one proposed by Freeman, Pucci, and Binsch for a somewhat related system.²⁶

Whether or not the potential energy surface depicted in Figure 2 is completely accurate, the fact that one can draw it at all raises some interesting questions. The key feature of the surface is that it has a single transition state that leads eventually to more than one product. In how many reactions does this occur? How would transition-state theory²⁷ or RRKM theory²⁸ deal with such a situation?

How should one characterize the role of the cyclopentane-1,3-diyl in this particular deazetization reaction? According to our calculations, some trajectories from **3** will pass through the cyclopentane-1,3-diyl structure, some will not. Does that make cyclopentane-1,3-diyl an intermediate in the deazetization of **1** or not? In general, how should one characterize a structure that resides at a local minimum on the potential energy surface, is energetically accessible, but is not on an obligatory path between reactant and products? Overall, would one say that the conversion of **3** to bicyclo[2.1.0]pentane involves concerted C-C bond formation and C-N bond cleavage or not?

Perhaps we have been forced into too dogmatic a classification of our reactions (concerted vs nonconcerted or single-step vs multistep) by the limitations of both our language and our models of mechanism.

Experimental Section

¹H NMR spectra were obtained on a Varian XL-200, Bruker WM-300, or Varian XL-400 FT spectrometer. ²H NMR spectra were obtained at 61.4 MHz on a Varian XL-400 FT spectrometer.

(26) Freeman, J. P.; Pucci, D. G.; Binsch, G. *J. Org. Chem.* **1972**, *37*, 1894.

(27) (a) Pelzer, H.; Wigner, E. *Z. Physik. Chem.* **1932**, *B15*, 445. (b) Glasstone, S.; Laidler, K. J.; Eyring, H. *Theory of Rate Processes*; McGraw-Hill: New York, 1940.

(28) (a) Rice, O. K.; Ramsperger, H. C. *J. Am. Chem. Soc.* **1927**, *49*, 1617. (b) Rice, O. K.; Ramsperger, H. C. *J. Am. Chem. Soc.* **1928**, *50*, 617. (c) Kassel, L. S. *J. Phys. Chem.* **1928**, *32*, 225. (d) Kassel, L. S. *J. Phys. Chem.* **1928**, *32*, 1065. (e) Marcus, R. A.; Rice, O. K. *J. Phys. Colloid Chem.* **1951**, *55*, 894. (f) Marcus, R. A. *J. Chem. Phys.* **1952**, *20*, 359. (g) Robinson, P. J.; Holbrook, K. A. *Unimolecular Reactions*; Wiley: New York, 1971. (h) Forst, W. *Unimolecular Reactions*; Academic Press: New York, 1973.

Cyclopropylmethanol, 4-(dimethylamino)pyridine, *p*-toluenesulfonyl chloride, potassium *tert*-butoxide, ethyl diazoacetate, phenyllithium, sodium amide, methanol-*d*, and deuterium oxide were obtained from commercial sources (Aldrich Chemical Company) and were used without purification. Pyridine, carbon disulfide, and dimethyl sulfoxide were distilled from calcium hydride. Toluene and diethyl ether were distilled from sodium benzophenone ketyl. Methyl acetate was triply distilled from phosphorus pentoxide.

2,3-Diazabicyclo[2.2.1]hept-2-ene-*exo,exo*-5,6- d_2 (**1**). The procedure of Gassman and Mansfield²⁹ was followed, except that deuterium was used in place of hydrogen in the catalytic hydrogenation step: ¹H NMR (200 MHz, acetone-*d*₆) δ 0.74 (d, $J = 1.9$ Hz, 2 H), 1.06 (dtt, $J = 10.5$, 2.0, 2.0 Hz, 1 H), 1.16 (d, $J = 10.5$ Hz, 1 H), 5.05 (d, $J = 2.0$ Hz, 2 H); ²H NMR (61.4 MHz, C₆D₆) δ 0.79.

1,3-Cyclopentadiene-1,2,3,4,5,5- d_6 . Cyclopentadiene-*d*₆ was synthesized according to the procedure of Lambert and Finzel.³⁰ A 10% NaOD-D₂O solution was prepared by adding Na (11 g) in portions to 100 mL of D₂O cooled to 0 °C. Freshly cracked 1,3-cyclopentadiene (8.8 g, 11.0 mL, 0.133 mol) was dissolved in DMSO (12 mL) in a 50-mL round-bottomed flask. A portion of the NaOD-D₂O solution (13 mL) was added to the reaction flask, and the mixture was stirred vigorously under dry N₂ for 1 h. The reaction mixture was then transferred to a 60-mL separatory funnel resulting in the formation of three layers. The lower two layers were removed and the upper cyclopentadiene layer was transferred via pipet to a clean 50-mL, round-bottomed flask. The exchange process was repeated five times, resulting in six total exchanges. After the final exchange, the crude cyclopentadiene was placed in a clean 10-mL, round-bottomed flask and was flash distilled with a heat gun through a short-path condenser into an ice-cooled receiver to give cyclopentadiene-*d*₆ (4.33 g, 5.4 mL, 60 mmol) in 45% yield.

Diethyl 2,3-Diazabicyclo[2.2.1]hept-5-ene-2,3-dicarboxylate-1,4,5,6,7,7- d_6 . A solution of diethyl azodicarboxylate (1.45 g, 7.7 mL, 49 mmol) in anhydrous ether (20 mL) was placed in a 100-mL, round-bottomed flask. The solution was cooled with stirring to 0 °C under a N₂ atmosphere. A solution of cyclopentadiene-*d*₆ (4.33 g, 60 mmol) in 20 mL of anhydrous ether was maintained at 0 °C and was transferred in portions via cannula to the reaction flask over a 45-min period. Stirring was continued for 3 h upon completion of the addition. The solvent was then removed on a rotary evaporator and the crude product was distilled bulb-to-bulb (0.2 Torr and 120 °C) to give 11.36 g (46 mmol) of pure material in 95% yield. Analysis by ¹H NMR showed total deuterium incorporation of 95%: ¹H NMR (200 MHz, CDCl₃) δ 4.19 (q, $J = 7.1$ Hz, 4 H) 1.26 (t, $J = 7.2$ Hz, 6 H).

Diethyl 2,3-Diazabicyclo[2.2.1]heptane-2,3-dicarboxylate-endo-endo-1,4,5,6,7,7- d_6 . Diethyl 2,3-diazabicyclo[2.2.1]hept-5-ene-2,3-dicarboxylate-1,4,5,6,7,7-*d*₆ (11.36 g, 46 mmol) was dissolved in absolute EtOH (100 mL) in a high-pressure bottle. A catalytic amount (200 mg) of 10% Pd/C was added, and the mixture was shaken for 20 h under 55 psi of H₂ on a Parr hydrogenator. The mixture was filtered through a 1-cm Celite pad, and the solvent was removed on a rotary evaporator to give the desired product (10 g, 40 mmol) in 87% yield. The material was used without further purification: ¹H NMR (200 MHz, CDCl₃) δ 4.19 (q, $J = 6.9$ Hz, 4 H), 1.26 (t, $J = 7.2$ Hz, 6 H).

2,3-Diazabicyclo[2.2.1]hept-2-ene-1,4,5,6,7,7- d_6 (**4**). A three-necked, 100-mL, round-bottomed flask equipped with a reflux condenser, a N₂ inlet, and a thermometer was charged with ethylene glycol (30 mL). Dry N₂ was bubbled through the solution for 10 min. The liquid was warmed to 45 °C in an oil bath, and KOH (5.0 g, 89.1 mmol) was added. The stirred solution was warmed to 125 °C under a N₂ atmosphere and a solution of diethyl 2,3-diazabicyclo[2.2.1]heptane-2,3-dicarboxylate-endo-endo-1,4,5,6,7,7-*d*₆ (5 g, 20 mmol) in ethylene glycol (5 mL) was added. The solution was maintained at 125 °C for 90 min. After cooling to room temperature, the solution was stirred for an additional 26 h. The solution was then poured into a mixture of concentrated HCl (9 mL) and ice water (40 mL). The solution was heated at 40 °C for 15 min (until gas evolution ceased) and was cooled to room temperature. The solution was adjusted to pH 7 with 6 M aqueous NH₃. A 2 M CuCl₂ solution (20 mL) was added in four 5-mL portions. After each addition, the solution was adjusted to pH 7 with additional ammonia, and the red-brown copper complex was collected on a Büchner funnel. The combined precipitated material was washed successively with 20% aqueous NH₄Cl (2 × 25 mL), 93% EtOH (2 × 5 mL), and cold H₂O (2 × 5 mL). The copper complex was air dried and transferred to a liquid-liquid continuous extractor. A solution of NaOH (1.16 g, 29 mmol) in H₂O (10 mL) was added to the complex, resulting in the formation of a gelatinous brown precipitate. The solution was saturated with NaCl and was subjected to continuous extraction with pentane (150 mL) for 70 h. After

(29) Gassman, P. G.; Mansfield, K. T. *Org. Synth.* **1969**, *49*, 1.

(30) Lambert, J.; Finzel, R. *J. Am. Chem. Soc.* **1983**, *105*, 1957.

drying over a mixture of K_2CO_3 and $MgSO_4$, the pentane was removed on a rotary evaporator to give the crude azo compound (1.58 g, 15.5 mmol) in 77% yield. Purification was achieved by successive sublimation, elution through a 10-cm Florisil column with 1:1 hexanes-ether, and resublimation. Pure 2,3-diazabicyclo[2.2.1]hept-2-ene-1,4,5,6,7,7-d₆ (0.70 g) was obtained in 34% yield: 1H NMR (200 MHz, $CDCl_3$) δ 1.49 (s), 2H NMR (400 MHz, 1 drop C_6D_6 in CS_2) δ 4.80 (2 H), 0.87 (1 H), 0.80 (1 H), 0.65 (2 H).

Cyclobutanol. Cyclobutanol was prepared by a modified procedure of Salaün and Fadel.³¹ In a typical procedure, a three-necked, 500-mL, round-bottomed flask equipped with a magnetic stirrer and reflux condenser was charged with 250 mL of water and 25 mL of 12 M hydrochloric acid. Cyclopropylmethanol (25 g, 0.35 mol) was added, and the stirred solution was heated for 3 h at reflux. After cooling to room temperature, the solution was saturated with NaCl and was subjected to continuous extraction with 400 mL of diethyl ether for 34 h. The extract was dried over $MgSO_4$, and the ether was removed by distillation through a 20-cm Vigreux column at atmospheric pressure to yield 20.5 g of crude product. Analysis by 1H NMR indicated a mixture of the desired cyclobutanol (89%) and 3-buten-1-ol (11%). The mixture was dissolved in 100 mL of pentane and was cooled to 0 °C. Bromine (4.76 g, 29.8 mmol) was added with vigorous stirring. After 5 min, the solution was transferred to a separatory funnel and was washed successively with saturated aqueous $NaHSO_3$ (25 mL) and saturated aqueous NaCl (25 mL). After drying over $MgSO_4$, the solvent was removed by distillation through a 20-cm Vigreux column. Distillation of the product through a short-path condenser afforded pure cyclobutanol (14.9 g) as a colorless liquid. Typical yields ranged from 60–63%: 1H NMR (200 MHz, $CDCl_3$) δ 4.17 (m, 1 H), 2.86 (s, 1 H, OH), 2.20 (m, 2 H), 1.85 (m, 2 H), 1.59 (m, 1 H), 1.37 (m, 1 H).

Cyclobutyl Tosylate. Into an oven-dried, three-necked, 500-mL, round-bottomed flask, equipped with a magnetic stirrer, was placed cyclobutanol (32.2 g, 0.45 mol) and dry pyridine (120 mL). 4-(Dimethylamino)pyridine (2.73 g, 0.022 mol, 0.05 equiv) was added, and the stirred solution was cooled to 0 °C in an ice bath. *p*-Toluenesulfonyl chloride (80 g, 0.42 mol) was added in portions over a 15-min period. Stirring was continued for 1 h at 0 °C. The solution was then warmed to room temperature and was stirred an additional 22 h. The reaction mixture was poured into a 2000-mL Erlenmeyer flask containing a 3 M solution of hydrochloric acid (100 mL) at 0 °C. The resulting mixture was divided into two equal portions. Each was extracted with three 100-mL portions of diethyl ether. The combined ethereal extracts were washed successively with H_2O (3 \times 100 mL), saturated aqueous $NaHCO_3$ (2 \times 50 mL), and saturated aqueous NaCl (1 \times 50 mL). After drying over $MgSO_4$, the ether was removed on a rotary evaporator and the product was further concentrated under vacuum (0.01 Torr) to remove unreacted cyclobutanol. Cyclobutyl tosylate (88.02 g, 0.389 mol) was obtained in 87% yield. Typical yields varied between 80% and 87%: 1H NMR (200 MHz, $CDCl_3$) δ 7.77 (d, J = 8.19 Hz, 2 H), 7.32 (d, J = 8.5 Hz, 2 H), 4.77 (quintet, J = 7.5 Hz, 1 H), 2.42 (s, 3 H), 2.17 (m, 4 H), 1.75 (m, 1 H), 1.5 (quintet, J = 7.5 Hz, 1 H).

Cyclobutene. An oven-dried, 250-mL, round-bottomed flask was equipped with a magnetic stirrer, a reflux condenser, and a pressure-equalizing addition funnel. Two cold-finger traps containing loosely packed glass wool were connected in series to the reflux condenser via a 3-cm section of Tygon tubing attached to the top of the reflux condenser. A stream of dry N_2 was introduced via a septum inlet positioned at the top of the addition funnel. The stream exited through a mineral oil bubbler connected to the second cold finger. The traps were cooled to -78 °C in a dry ice-acetone bath, and the reaction flask was charged with DMSO (120 mL) and potassium *tert*-butoxide (33.6 g, 0.30 mol). The stirred suspension was heated to 70 °C in an oil bath, and a solution of cyclobutyl tosylate (25.6 g, 0.113 mol) in DMSO (30 mL) was placed in the addition funnel and added over a 10-min period. Stirring and heating at 70 °C was continued for 2 h. The tubing connecting the condenser to the first cold finger was then replaced with a N_2 inlet, isolating both traps from the reaction apparatus. A slow N_2 purge was continued, and the dry ice-acetone bath was removed from the first cold trap allowing pure cyclobutene to distill into the second trap. The second trap containing the product was then isolated and kept at -78 °C until needed. The cyclobutene obtained was used without further purification.

exo- and endo-Ethyl Bicyclo[2.1.0]pentane-5-carboxylates.³² An oven-dried, three-necked, 100-mL, round-bottomed flask was taken into a glovebox and charged with bis[copper(I) trifluoromethanesulfonate]-benzene complex³³ (0.95 g). The flask was fitted with a

Dewar condenser in the center neck and rubber septa in the remaining necks and was removed from the glovebox. A N_2 inlet was introduced through a rubber septum attached to the condenser. The Dewar condenser and the reaction vessel were both cooled to -78 °C with a dry ice-acetone mixture. Methyl acetate (30 mL) was transferred to the reaction flask via cannula. Cyclobutene was then transferred to the reaction flask by connecting the chilled vessel containing the cyclobutene to the reaction flask with a stainless-steel cannula and then allowing the vessel to warm to room temperature. The stirred copper triflate-cyclobutene solution was maintained at -10 °C in a NaCl-MeOH-ice mixture. Ethyl diazoacetate (6.85 g, 6.3 mL, 0.06 mol) was added over a 150-min period with a syringe pump. The reaction mixture was then allowed to warm to room temperature, and stirring was continued for an additional 4 h. The reaction mixture was poured into a separatory funnel containing 100 mL of saturated aqueous NH_4Cl , and aqueous NH_3 was added to adjust the solution to pH 9. The mixture was extracted with three 75-mL portions of ether. The extracts were washed successively with H_2O (3 \times 100 mL) and saturated aqueous NaCl solution (50 mL). After drying over $MgSO_4$, the solvent was removed by distillation through a 10-cm Vigreux column. The crude product was purified by elution down a silica gel column with 20% ethyl acetate in hexanes. A mixture of endo and exo isomeric esters (4.20 g, 0.030 mol) were obtained in 50% yield based on ethyl diazoacetate as the limiting reagent. Yields for the two-step sequence averaged 30%: 1H NMR (200 MHz, $CDCl_3$) exo isomer δ 4.09 (q, J = 6.9 Hz, 2 H), 2.10–2.28 (m, 2 H), 2.03 (br s, 2 H), 1.76 (s, 1 H), 1.43–1.53 (m, 2 H), 1.24 (t, J = 6.9 Hz, 3 H).

endo- and exo-Bicyclo[2.1.0]pentane-5-carboxylic Acids.³² A 1000-mL, round-bottomed flask equipped with a reflux condenser was charged with a mixture of endo- and exo-ethylbicyclo[2.1.0]pentane-5-carboxylates (6.01 g, 0.043 mol) in 400 mL of 80% aqueous ethanol. NaOH (21.5 g, 0.53 mol) was added and the stirred solution was heated for 10 h at reflux. After cooling to 0 °C in an ice bath, the solution was acidified to pH 2 by the addition of 50 mL of concentrated HCl. The solution was extracted with four 100-mL portions of ether. The combined extracts were washed with 50 mL of saturated aqueous NaCl solution and were dried over $MgSO_4$. After removal of the solvent on a rotary evaporator, the crude solid was distilled bulb-to-bulb (0.2 Torr, 100 °C) to give bicyclo[2.1.0]pentane-5-carboxylic acid (4.38 g, 0.039 mol) in 91% yield as a mixture of endo and exo isomers. *The carboxylic acid product has an extremely unpleasant odor and manipulations should be conducted in a good fume hood.* 1H NMR (200 MHz, $CDCl_3$) exo isomer δ 2.18–2.30 (m, 2 H), 2.11 (br s, 2 H), 1.76 (s, 1 H), 1.49–1.54 (m, 2 H).

endo- and exo-5-Benzoylbicyclo[2.1.0]pentanes.³² An oven-dried, 100-mL, round-bottomed flask equipped with a strong magnetic stirrer was charged with a solution of a mixture of endo- and exo-bicyclo[2.1.0]pentane-5-carboxylic acids (1.75 g, 16 mmol) in 50 mL of dry ether. The stirred solution was cooled to 0 °C under a N_2 atmosphere and PhLi (20 mL of 1.8 M solution in hexanes-ether, 36 mmol, 2.3 equiv) was added via syringe. The mixture was stirred for 1 h and was poured into a separatory funnel containing 100 mL of saturated aqueous NH_4Cl . The resulting mixture was extracted with three 100-mL portions of ether. The combined ethereal extracts were washed successively with H_2O (50 mL), saturated aqueous $NaHCO_3$ (50 mL), and saturated aqueous NaCl (50 mL). Drying over $MgSO_4$ and removal of the solvent on a rotary evaporator afforded the desired product contaminated with biphenyl and the product of the addition of a second equivalent of PhLi. The crude ketone was used without purification.

exo-5-Benzoylbicyclo[2.1.0]pentane-endo-5-d.³² A $NaOCH_3-CH_3OD$ solution was prepared by adding Na (2.2 g, 96 mmol) in portions to 70 mL of CH_3OD (99.5% D) cooled to 0 °C in an ice bath under a N_2 atmosphere. An oven-dried, 100-mL, round-bottomed flask was charged with the crude 5-benzoylbicyclo[2.1.0]pentane and 35 mL of the $NaOCH_3-CH_3OD$ solution. A reflux condenser was attached, and the stirred solution was heated at reflux under N_2 for 8 h. After cooling to room temperature, the mixture was poured into a separatory funnel containing 100 mL of H_2O and was extracted with three 40-mL portions of ether. The combined ethereal extracts were dried over $MgSO_4$, and the solvent was removed on a rotary evaporator. The residue was subjected to a second D/H exchange with the remaining $NaOCH_3-CH_3OD$ solution. Workup as before provided the crude deuterated material with greater than 99% deuterium incorporation as indicated by 1H NMR analysis. Purification by column chromatography (5% THF in hexanes on silica gel) provided pure exo-5-benzoylbicyclo[2.1.0]pentane-endo-5-d (1.71 g, 9.9 mmol) in 63% yield from bicyclo[2.1.0]pentane-5-carboxylic acids: 1H NMR (200 MHz, $CDCl_3$) δ 8.00–8.05 (m, 2 H), 7.47–7.57 (m, 3 H), 2.25–2.40 (m, 4 H), 1.64–1.68 (m, 2 H).

Bicyclo[2.1.0]pentane-endo-5-d.³² An oven-dried, three-necked, 100-

(31) Salaün, J.; Fadel, A. *Organic Syntheses*; Wiley: New York, 1990; Collect. Vol. VII, p 118.

(32) Wiberg, K. B.; Kass, S. R.; Bishop, K. C. *J. Am. Chem. Soc.* 1985, 107, 996.

(33) Saloman, R. G.; Kochi, J. K. *J. Am. Chem. Soc.* 1973, 95, 1889.

mL, round-bottomed flask equipped with a reflux condenser and N₂ inlet was charged with NaNH₂ (5.0 g, 128 mmol, 12.6 equiv) and dry toluene (50 mL). The top of the condenser was connected to a dry ice-acetone-cooled cold-finger trap (packed loosely with glass wool) with a 2-cm section of Tygon tubing. A slow stream of dry N₂ was introduced into the reaction flask through the N₂ inlet and exited through the cold trap via a mineral oil bubbler. A solution of *exo*-5-benzoylbicyclo[2.1.0]pentane-*endo*-5-*d* (1.75 g, 10.1 mmol) in toluene (10 mL) was added to the reaction flask via syringe, and the stirred suspension was heated at reflux. After 3 h, the heat was removed, and the cold trap was connected directly to the reaction flask by removal of the reflux condenser. When the reaction flask had cooled to room temperature, the cold finger was isolated from the apparatus, and the bicyclopentane was stored at -78 °C.

endo-4-Phenyl-2,4,6-triazatricyclo[5.2.1.0^{2,6}]decane-3,5-dione-syn-10-*d*. This urazole was prepared by the method of Dougherty et al.³⁴ *N*-Phenyl-1,2,4-triazoline-3,5-dione³⁵ (1.77 g, 10.1 mmol) was placed in a 100-mL, round-bottomed flask equipped with a water-cooled spiral condenser. A dry ice-acetone-cooled Dewar condenser was placed on top of the spiral condenser and the reaction apparatus was purged with dry N₂. Bicyclo[2.1.0]pentane-*endo*-5-*d* was transferred from its chilled container to the reaction flask with five 10-mL portions of hexanes. The reaction mixture was heated for 3 h at reflux and was allowed to cool to room temperature. Purification was achieved by elution down a 45-mm silica gel column with 1:1 hexanes/ethyl acetate. Pure *endo*-4-phenyl-2,4,6-triazatricyclo[5.2.1.0^{2,6}]decane-3,5-dione-*syn*-10-*d* (250 mg, 1.02 mmol) was obtained in a combined 10% yield for the two steps from 5-benzoylbicyclo[2.1.0]pentane. Alternatively, conducting the reaction in isooctane solution in a sealed tube resulted in a 3% yield: ¹H NMR (200 MHz, CDCl₃) δ 7.37-7.47 (m, 5 H), 4.67 (br s, 2 H), 1.78-2.00 (m, 5 H).

2,3-Diazabicyclo[2.2.1]hept-2-ene-*endo*-7-*d* (5). A 100-mL, round-bottomed flask equipped with a reflux condenser was charged with a 1:1 mixture of 2-propanol and methanol (35 mL). The solution was deoxygenated with a N₂ purge for 15 min. KOH (1.4 g, 25 mmol) and *endo*-4-phenyl-2,4,6-triazatricyclo[5.2.1.0^{2,6}]decane-3,5-dione-*syn*-10-*d*

(300 mg, 1.23 mmol) were added successively. The stirred solution was heated for 18 h at reflux under a N₂ atmosphere. After cooling to room temperature, the solution was acidified to pH 2 with concentrated HCl and then heated at 70 °C for 5 min to effect decarboxylation. After neutralization to pH 7 with 6 N aqueous ammonia and cooling to 0 °C in an ice bath, 2 mL of a 1 M aqueous CuCl₂ solution was added. The solution was readjusted to pH 7 with additional ammonia, resulting in the precipitation of the brick-red copper-azo complex. Stirring was continued for 15 min, and the complex was collected in a Büchner funnel. The complex was washed with two 1-mL portions of ice-cold saturated aqueous NaCl solution and was transferred to a 60-mL separatory funnel. The complex was decomposed by the addition of 10 mL of a 6 N aqueous NH₃ solution. The blue solution was extracted with four 10-mL portions of ether. The combined extracts were washed successively with H₂O (10 mL) and saturated aqueous NaCl (10 mL) and were dried over Na₂SO₄. After decantation from the drying agent, the solution was heated to 70 °C in an oil bath and the ether was removed by distillation through a 10-cm column packed with glass helices. When the volume had been reduced to approximately 1 mL, pentane (10 mL) was added, and the distillation was continued. When the volume had again been reduced to 1 mL, the distillation flask was removed, and its contents cooled to -78 °C under a N₂ atmosphere, resulting in precipitation of the azo compound. The supernatant was removed by decantation. Residual pentane was removed by warming the flask in an oil bath at 50 °C for 5 min. 2,3-Diazabicyclo[2.2.1]hept-2-ene-*endo*-7-*d* (5) (43 mg, 0.44 mmol) was obtained in 36% yield. Analysis by ¹H NMR showed the presence of a minor unidentified impurity. The impurity was chemically inert under pyrolysis conditions and contained no deuterium as was evident from the ²H NMR spectrum of the azo compound: ¹H NMR (200 MHz, CDCl₃) δ 5.35 (br s, 2 H), 1.70-1.90 (m, 2 H), 1.40 (s, 1 H), 1.13-1.30 (m, 2 H).

Acknowledgment. We thank Professor Gregory Ezra for bringing ref 24a and b to our attention. The theoretical work was conducted using the Cornell National Supercomputer Facility, a resource Center for Theory and Simulations in Science and Engineering (Cornell Theory Center), which receives major funding from the National Science Foundation and IBM Corporation, with additional support from New York State and members of the Corporate Research Institute.

(34) Jain, R.; Sponsler, M. B.; Coms, F. D.; Dougherty, D. D. *J. Am. Chem. Soc.* **1988**, *110*, 1356.

(35) Stickler, J. C.; Pirkle, W. H. *J. Org. Chem.* **1966**, *31*, 3444.

Electron Transfer in Di(deoxy)nucleoside Phosphates in Aqueous Solution: Rapid Migration of Oxidative Damage (via Adenine) to Guanine

Luis Pedro Candeias and Steen Steenken*

Contribution from the Max-Planck-Institut für Strahlenchemie, D-4330 Mülheim, Germany.

Received August 3, 1992

Abstract: In aqueous solution, the one-electron loss centers created statistically by the oxidant SO₄^{•-} or by photoionization in di(2'-deoxy)nucleoside phosphates (DNPs) containing the base guanine (G) become localized at G, as concluded from pulse radiolysis and 193-nm laser photolysis experiments. From the latter it is evident that, in the case of adenylyl(3'→5')guanosine (ApG), the charge-transfer process is complete in ≤50 ns. With DNPs containing a pyrimidine and the purine base adenine, the oxidative damage is collected by the adenine moiety ($k \geq 2 \times 10^5 \text{ s}^{-1}$).

Introduction

It has long been known that the electron loss centers created in DNA^{1,2} or DNA model compounds^{3,4} by ionizing radiation or

other oxidizing agents ultimately end up at guanine (G). Since with ionizing radiation the initial distribution of the electron loss centers is of statistical nature, it was proposed that the "positive holes" migrate along (or across)⁵ the stacked bases of DNA until

(1) For reviews see, e.g.: Hüttermann, J.; Köhnlein, W.; Teoule, R.; Bertinchamps, A. J., Eds. *Effects of Ionizing Radiation on DNA*; Springer: Berlin, 1978. Simic, M. G.; Grossman, L.; Upton, A. C., Eds. *Mechanisms of DNA Damage and Repair*; Plenum: New York, 1986. Bernhard, W. A. *Adv. Radiat. Biol.* **1981**, *9*, 199. Symons, M. C. R. *J. Chem. Soc., Faraday Trans. 1* **1987**, *83*, 1. Close, D. M.; Nelson, W. H.; Sagstuen, E. In *Electronic Magnetic Resonance of the Solid State*; Weil, J. A., Ed.; Canadian Society for Chemistry; Ottawa, 1987; p 237. Hüttermann, J. In *Radical Ionic Systems*; Lund, A.; Shiotani, M., Eds.; Kluwer: Dordrecht, 1991; p 435. For a recent report, see: Sevilla, M. D.; Becker, D.; Yan, M.; Summerfield, S. R. *J. Phys. Chem.* **1991**, *95*, 3409.

(2) (a) Al-Kazwini, A. T.; O'Neill, P.; Fielden, E. M.; Adams, G. E. *Radiat. Phys. Chem.* **1988**, *32*, 385. Al-Kazwini, A. T.; O'Neill, P.; Adams, G. E.; Fielden, E. M. *Radiat. Res.* **1990**, *121*, 149. (b) Hildenbrand, K.; Schulte-Frohlinde, D. *Free Radical Res. Commun.* **1990**, *11*, 195. (c) Candeias, L. P.; O'Neill, P.; Jones, G. D. D.; Steenken, S. *Int. J. Radiat. Biol.* **1992**, *61*, 15.

(3) Gregoli, S.; Olast, M.; Bertinchamps, A. *Radiat. Res.* **1977**, *70*, 255; *Ibid.* **1979**, *77*, 417.

(4) Sevilla, M. D.; D'Arcy, J. B.; Morehouse, K. M.; Engelhardt, M. L. *Photochem. Photobiol.* **1979**, *29*, 37.